

# Magnetic phase transitions in antiferromagnetic NiCO<sub>3</sub>

A. N. Bazhan

Institute of Physical Problems, USSR Academy of Sciences

(Submitted September 18, 1973)

Zh. Eksp. Teor. Fiz. 66, 1086-1099 (March 1974)

The magnetic properties of the antiferromagnetic crystal NiCO<sub>3</sub> were investigated with a vibrating-sample magnetometer in the temperature range 4.2–80 °K and for different directions of the magnetic field  $H$  ( $H_{\max} = 65$  kOe). The magnetic moment components parallel and perpendicular to the applied magnetic field were measured. It was found that at  $T = 4.2$  °K and for  $H = 0$ , the antiferromagnetic vector  $L$  is inclined at an angle  $\theta_0 = (68 \pm 2)^\circ$  to the trigonal axis. In an external magnetic field  $H \perp C_3$ ,  $L$  turns towards the basal plane (i.e., the plane perpendicular to the  $C_3$  axis) as  $H$  is increased from zero, reaching this plane when  $H = H_c = 14$  kOe. With  $H = 0$ , the crystal, upon increase of the temperature, goes over near the transition point  $T_N$  to a purely antiferromagnetic state (i.e., a state without weak ferromagnetism) in which  $L$  is directed along the trigonal axis. On application of a magnetic field  $H \sim 10$  kOe in a direction perpendicular to the  $C_3$  axis, the crystal goes over to a weakly ferromagnetic state with the magnetic moment lying in the basal plane.

Nickel carbonate is isomorphous to the well-investigated manganese and cobalt carbonates, which are antiferromagnets with weak ferromagnetism. NiCO<sub>3</sub> has a rhombohedral structure with two molecules per unit cell and the space group  $D_{3d}^6$ . However, because of the difficulties encountered in the synthesis and growth of single crystals of NiCO<sub>3</sub>, its magnetic properties were not thoroughly investigated until very recently. The existence at  $T = 4.2$  °K of a spontaneous ferromagnetic moment in NiCO<sub>3</sub> was discovered by Bizette and Tsai<sup>[1]</sup>. Later, Alikhanov<sup>[2]</sup> found in a neutron-diffraction study that below 25 °K NiCO<sub>3</sub> goes over into an antiferromagnetic state that, according to Dzyaloshinski's theory<sup>[3]</sup>, admits of weak ferromagnetism. Prozorova<sup>[4]</sup> has investigated the magnetic resonance properties of NiCO<sub>3</sub>, while Kreines and Shal'nikova<sup>[5]</sup> have investigated its static magnetic properties in comparatively weak fields  $H < 14$  kOe. The purpose of the present work was to investigate the anisotropy in the static magnetic properties of NiCO<sub>3</sub> in strong fields of up to 60 kOe. We used for these investigations samples obtained by Sthernberg and Minenzon<sup>[6]</sup> at the Crystallography Institute of the USSR Academy of Sciences<sup>[1]</sup>.

The measurements were performed with a modified vibrating-sample magnetometer<sup>[7]</sup>, which allowed the measurement of the magnetization of the sample in three mutually perpendicular directions. Figure 1 shows the disposition scheme for the pickup loops. The sample could rotate about the vertical axis  $z$ , and the magnetic field was directed along the  $x$  axis. The field dependences of the sample's resultant magnetic moment  $M(H)$  measured with the aid of the loops at different temperatures were recorded on a two-coordinate potentiometer. The measurements were performed from 4.2 to 80 °K. The magnetic field was produced by a superconducting solenoid. The measurements were performed for two sample positions: when the sample was fixed in such a way that the trigonal axis was directed along the vertical ( $z$ ) axis ( $H \perp C_3$ ), and when the trigonal axis was directed perpendicularly to the vertical axis. The error in the orientation of the sample relative to the pickup loops was 2–3°. The absolute sample temperature in the intermediate temperature range was measured to within 0.5°.

## RESULTS OF THE MEASUREMENTS

### 1. Temperature $T = 4.2^\circ$ K

Figure 2 (curve 1) shows the magnetization curve  $M_{\parallel}(H)$  for sample magnetization along the magnetic field

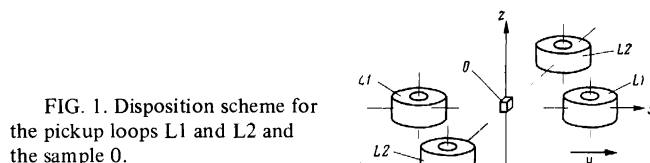


FIG. 1. Disposition scheme for the pickup loops L1 and L2 and the sample 0.

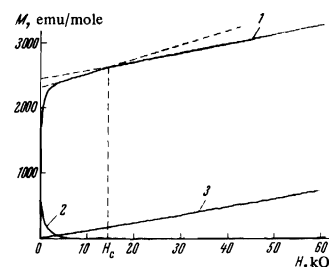


FIG. 2. Magnetization curves for NiCO<sub>3</sub>: curve 1— $M_{\parallel}(H)$  with  $H$  in the (001) plane; curve 2— $M_{\perp}(H)$  with  $H \perp C_2$  in the (001) plane; curve 3— $M_{\parallel}(H)$  with  $H \parallel [001]$ .

when the field is directed perpendicularly to the twofold axis  $C_2$  in the (001) plane (the  $M_{\parallel}(H)$  signal is tapped in this case from the coils L1 of the instrument (see Fig. 1)). It can be seen from the figure that the curve  $M_{\parallel}(H)$  has a kink at  $H = H_c = 14$  kOe resulting in a change in the slope of the magnetization curve: the slope of the curve decreases by a factor of two. The magnetization curve in the region  $H < H_c = 14$  kOe is sufficiently well described by the expression

$$M_{\parallel}^I(H) = \sigma_{D_{\perp}}^I + \chi_{\perp}^I H, \quad (1)$$

and in the region  $H > H_c$  by the expression

$$M_{\parallel}^{II}(H) = \sigma_{D_{\perp}}^{II} + \chi_{\perp}^{II} H, \quad (2)$$

where  $M_{\parallel}^I(H)$ ,  $M_{\parallel}^{II}(H)$  and  $\chi_{\perp}^I$ ,  $\chi_{\perp}^{II}$  are the resultant magnetic moments and the magnetic susceptibilities in the basal plane (001) respectively for  $H < H_c$  and  $H > H_c$ ;  $\sigma_{D_{\perp}}^I$  and  $\sigma_{D_{\perp}}^{II}$  are the corresponding ferromagnetic moments. The values of  $\sigma_{D_{\perp}}$  are obtained by extrapolating the linear sections of the strong-field magnetization curves to  $H = 0$ . We then have from the experiment

$$\sigma_{D_{\perp}}^I / \sigma_{D_{\perp}}^{II} = 0.94 \pm 0.01, \quad \chi_{\perp}^I / \chi_{\perp}^{II} = 1.6 \pm 0.2, \quad (3)$$

$$\sigma_{D_{\perp}}^I = (2300 \pm 40) \text{ emu/mole}, \quad \sigma_{D_{\perp}}^{II} = 2340 \pm 40 \text{ emu/mole},$$

$$\chi_{\perp}^I = (26.4 \pm 1) \cdot 10^{-3} \text{ emu/mole}, \quad \chi_{\perp}^{II} = (16.8 \pm 1) \cdot 10^{-3} \text{ emu/mole}.$$

The values  $\sigma_{D_{\perp}}^I$  and  $\chi_{\perp}^I$  agree fairly well with the data of<sup>[5]</sup>:  $\sigma_{D_{\perp}} = 2880$  emu/mole and  $\chi_{\perp} = (23.8 \pm 1) \times 10^{-3}$  emu/mole.

The experiments showed that the shape of the magnetization curve  $M_{\parallel}(H)$  was, to within the limits of the experimental error, independent of the direction of the magnetic field  $H$  in the (001) plane.

The curve 2 of Fig. 2 shows the dependence  $M_{\perp}(H)$  when the magnetic field  $H$  is directed perpendicularly to the twofold axis in the (001) plane (the  $M_{\perp}(H)$  signal is tapped from the coils L2 of the instrument (see Fig. 1)). It can be seen that  $M_{\perp}(H)$  is different from zero at  $H=0$  and in weak fields. However, as the magnetic field is increased,  $M_{\perp}(H)$  decreases, and is equal to zero for  $H > 7-8$  kOe. This behavior of  $M_{\perp}(H)$  is connected with the fact that at  $H=0$  the crystal is divided into domains with the spontaneous magnetizations directed along the six directions of the twofold axes in the (001) plane. In the solenoid's weak remanent magnetic field  $H \sim 200$  Oe directed perpendicularly to one of the  $C_2$  axes, the crystal is remagnetized into two domain regions with the spontaneous magnetic moments directed along twofold axes, along the magnetic field. In the process, a significant signal is induced in the coil L2 of the instrument. Upon subsequent increase of the magnetic field, the crystal goes over into a single-domain state with the spontaneous magnetic moment oriented parallel to the applied magnetic field; in this case  $M_{\perp}(H) = 0$ . It can be seen from Fig. 2 (curve 2) that the crystal goes over into the single-domain state when  $H > 7-8$  kOe. Thus, the kink in the magnetization curve  $M_{\parallel}(H)$  (curve 1), which occurs at  $H = H_C = 14$  kOe, is not connected with the transition of the crystal to the single-domain state.

We also used in the investigations pickup loops that measured the spontaneous magnetic moment in the vertical ( $z$ ) direction (see Fig. 1). We did not in this experiment detect a significant ( $\approx 5\%$   $\sigma_{D\perp}$ ) spontaneous magnetic moment component along the trigonal axis when  $H < H_C$ . In other words, the kink in the magnetization curve  $M_{\parallel}(H)$  (Fig. 2, curve 1) at  $H = H_C$  is also not connected with the existence of some spontaneous magnetic moment components perpendicular to the magnetic field  $H$ .

Thus, we can conclude from the foregoing that in fields  $H = H_C = 14$  kOe with  $H \perp C_3$ , there occurs in the ferromagnetic moment  $\sigma_{D\perp}$  of  $\text{NiCO}_3$  an increase that is due neither to the transition of the sample to the single-domain state nor to the existence in the sample of substantial spontaneous magnetic moment components perpendicular to the magnetic field, i.e.,  $\sigma_{D\perp}$  is oriented parallel to the applied magnetic field, and lies in the plane perpendicular to the trigonal axis. We can also conclude from the nondependence of the magnetization curve  $M_{\parallel}(H)$  on the direction of the magnetic field  $H$  in the (001) plane that the antiferromagnetic vector  $L$  in this case lies in the plane perpendicular to the spontaneous magnetic moment, i.e., in the plane perpendicular to the applied magnetic field  $H$ .

In Fig. 2 we also show the dependence of the magnetic moment  $M_{\parallel}(H)$  on the magnetic field for  $H \perp C_3$  (curve 3). In this case the  $H$  dependence of the magnetic moment of the sample has the form

$$M_{\parallel}(H) = \chi_{\perp} H, \quad \chi_{\perp} = (14.8 \pm 1) \cdot 10^{-3} \text{ emu/mole.} \quad (4)$$

## 2. The Temperature Region 4.2-80°K

The nature of the magnetization curves of  $\text{NiCO}_3$  changes as the temperature is increased. In Fig. 3 we show the field dependence of the magnetic moment  $M_{\parallel}(H)$

of the sample for different temperatures. It can be seen from the figure that in weak fields  $\sigma_{D\perp}^I(T)$  decreases more rapidly with increasing temperature than  $\sigma_{D\perp}^{II}(T)$ , and is equal to zero when  $T \geq 22.6$  °K, i.e., the linear dependence  $M_{\parallel}^I(H) = \sigma_{D\perp}^I(T) + \chi_{\perp}^I(T)H$  for  $H < 14$  kOe is fulfilled only at temperatures  $T < 22.6$  °K. When  $T > 22.6$  °K a nonlinear dependence of the magnetic moment on the applied magnetic field  $H \perp C_3$  is observed in weak fields. In Fig. 3 we show the dependence  $M_{\perp}(H)$  for the same direction of the magnetic field and for  $T > 22.6$  °K. It can be seen that  $M_{\perp}(H) \approx 0$  at  $H=0$ , i.e., the decrease of  $\sigma_{D\perp}^I$  to zero is not connected with the division of the sample into domains as the temperature is increased.

In a magnetic field  $H > H_C$  the dependence of the resultant magnetic moment of the sample on the applied magnetic field is described by the expression  $M_{\parallel}^{II}(H) = \sigma_{D\perp}^{II}(T) + \chi_{\perp}^{II}(T)H$  in the entire temperature range from 4.2 °K to  $T_N$ , where  $T_N$  was determined from the vanishing of the ferromagnetic moment  $\sigma_{D\perp}^{II}$ . Consequently, when  $H > H_C$  the crystal is a weak ferromagnet with the ferromagnetic moment directed along the magnetic field.

Thus, from the data shown in Fig. 3 we can draw the qualitative conclusion that as the temperature is increased in the absence of an external magnetic field (i.e., when  $H=0$ ), a  $\text{NiCO}_3$  single crystal goes over from a weakly-ferromagnetic state into a purely anti-ferromagnetic state at  $T \geq 22.6$  °K. Upon application of a magnetic field  $H > H_C$  with  $H \perp C_3$  the crystal goes over into a state possessing weak ferromagnetism, which, for  $H > H_C$ , is equal to  $\sigma_{D\perp}^{II}(T)$ .

Figure 4 shows the dependence  $\sigma_{D\perp}^{II}(T)$  of the ferromagnetic moment obtained by extrapolating to  $H=0$  the linear section observable in the  $H > H_C$  region of the magnetic-moment curves  $M_{\parallel}^{II}(H)$  for different temperatures, as well as the dependence  $\sigma_{D\perp}^I(T)$  obtained by extrapolating to  $H=0$  the linear section of the  $H < H_C$  region of the magnetic-moment curve  $M_{\parallel}^I(H)$ . It can be seen from the figure that the spontaneous moment  $\sigma_{D\perp}^I(T)$  decreases more rapidly with increasing  $T$  than  $\sigma_{D\perp}^{II}(T)$  and that  $\sigma_{D\perp}^I = 0$  at  $T_I \geq 22.6$  °K. The critical temperature for the transition to the antiferromagnetic state, which was determined from the vanishing of the

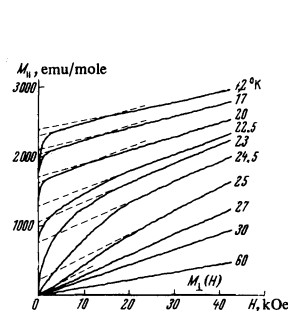


FIG. 3

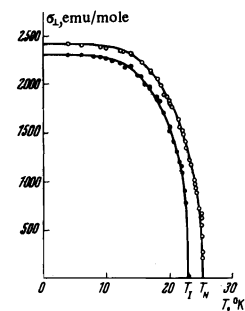


FIG. 4.

FIG. 3. Magnetization curves  $M_{\parallel}(H)$  at different temperatures, as well as the curve  $M_{\perp}(H)$ ;  $H \perp C_3$ .

FIG. 4. The temperature dependences of the ferromagnetic moments:  $\circ - \sigma_{D\perp}^I(T)$ ,  $\bullet - \sigma_{D\perp}^{II}(T)$ .

spontaneous magnetic moment  $\sigma_{D\perp}^{\text{II}}$ , was found to be equal in strong fields to  $T_N = 25.2$  °K.

Figure 5 shows the temperature dependences of the magnetic susceptibilities  $\chi_{\perp}^{\text{II}}(T)$  for  $H \perp C_3$  ( $H > H_C$ ) and  $\chi_{\perp}^{\text{I}}(T)$  for  $H \parallel C_3$ . It can be seen that the dependence  $\chi_{\perp}^{\text{II}}(T)$  has a sharp maximum in the vicinity of the transition point  $T_N$ . The critical temperature for the transition of the single crystal to the antiferromagnetic state, as determined from the maximum of  $\chi_{\perp}^{\text{II}}(T)$ , turned out to be also equal to  $T_N = 25.2$  °K, which coincides with the value obtained in [5]. The construction of the temperature dependence  $\chi_{\perp}^{\text{I}}(T)$  is made difficult by the appearance of a nonlinear field dependence of the magnetic moment  $M_{\parallel}^{\text{I}}(H)$  in the region  $H < H_C$ .

Figure 6 shows the dependence  $M_{\perp}(H)$  for different temperatures, when  $H$  makes some angle  $\psi$  with the direction of the  $C_3$  axis ( $\psi \approx 8^\circ$ ). At  $T = 4.2$  °K, the value of  $M_{\perp}(H)$  corresponds to the value of the spontaneous magnetic moment  $\sigma_{D\perp}^{\text{I}}$ . It follows from the geometry of such an alignment of the magnetic field and the pickup loops  $L_2$  that in the present case  $M_{\perp}(H) = \sigma_{D\perp} \cos 8^\circ + \frac{1}{2}A\chi_{\perp}H \sin 16^\circ$ , where  $A$  is a coefficient depending on the orientation of the antiferromagnetic vector  $L$  relative to the  $C_3$  axis. It can be seen from the figure that, to a good degree of accuracy,  $M_{\perp}(H) = \sigma_{D\perp}^{\text{I}}$ , i.e.,  $A < 1$ . Figure 6 also confirms the vanishing of the spontaneous magnetic moment  $\sigma_{D\perp}^{\text{I}}$  at  $T > T_I$ . Upon further increase of the temperature  $T > T_N$ , the moment  $M_{\perp}(H)$  vanishes for all values of the magnetic field  $H$ . Thus, we can also conclude from the experimental data presented in Fig. 6

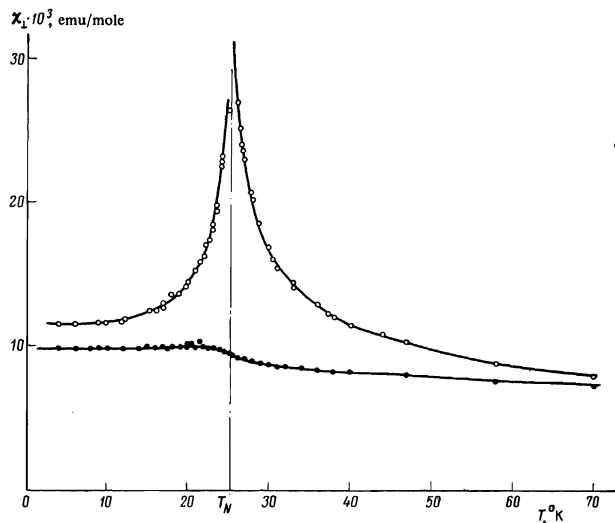


FIG. 5. The temperature dependences of the magnetic susceptibility:  $\circ - \chi_{\perp}^{\text{II}}(T)$  for  $H \perp C_3$  and  $H > H_C$ ;  $\bullet - \chi_{\perp}^{\text{I}}(T)$  for  $H \parallel C_3$ .

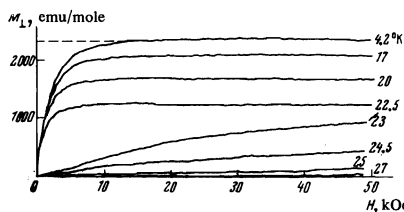


FIG. 6. Magnetization curves  $M_{\perp}(H)$  for  $H$  inclined at an angle  $\psi = 8^\circ$  to  $C_3$  and for different temperatures.

that for  $22.6$  °K  $< T < T_N$  and  $H = 0$  the crystal  $\text{NiCO}_3$  is a purely antiferromagnetic state, i.e., in an antiferromagnetic state without weak ferromagnetism. Upon application of a magnetic field, however, the crystal goes over into a state with weak ferromagnetism.

## DISCUSSION OF THE RESULTS

The nature of the  $\text{NiCO}_3$  magnetization curves can be explained on the basis of the theory, developed by Dzyaloshinskii [3], of weak ferromagnetism of antiferromagnets with the rhombohedral crystal structure. According to Dzyaloshinskii [3], the magnitude of the spontaneous magnetic moment  $\sigma_{D\perp}$  in the (001) plane linearly depends on the component of the antiferromagnetic vector  $L$  in this plane. Therefore, the obtained results can be explained on the basis of the following model.

Let us assume, in accordance with the neutron-diffraction data [2], that for  $H = 0$  and  $H < H_C$  the antiferromagnetic vector  $L$  is inclined at some angle  $\theta_0(T) \neq \pi/2$  to the threefold axis, and that this angle does not depend on the direction of the component of  $L$  in the (001) plane. As  $H \perp C_3$  is increased in magnitude from zero to  $H_C$ , the antiferromagnetic vector  $L$  turns toward the (001) plane, the rotation occurring in the plane perpendicular to the magnetic field  $H$  and being accompanied by the growth of the magnitude of the ferromagnetic moment  $\sigma_{D\perp} \parallel H$ . At  $H = H_C$  the antiferromagnetic vector  $L$  lies in the basal plane. The angle  $\theta_0(T)$  for  $H = 0$  is determined by the ferromagnetic-moment ratio  $\sigma_{D\perp}^{\text{I}}(T)/\sigma_{D\perp}^{\text{II}}(T)$ . As the temperature is increased,  $\theta_0$  decreases and is equal to zero at  $T \geq 22.6$  °K, i.e., the antiferromagnetic vector  $L$  is directed along the threefold axis, and the crystal does not possess a spontaneous magnetic moment.

The general form of the thermodynamic potential for the rhombohedral crystals with the symmetry group  $D_{3d}^5$  can be written in the form

$$\Phi = \frac{1}{2}a\gamma_z^2 + \frac{1}{2}Bm^2 - q(\gamma_x m_y - \gamma_y m_x) + \frac{1}{2}D(\gamma m)^2 + \frac{1}{2}bm_z^2 + \left[ \frac{1}{4}f\gamma_z^2 + \frac{1}{2}Rm^2 - r(\gamma_x m_y - \gamma_y m_x) \right] \gamma_z^2 - mH, \quad (5)$$

where  $\gamma = L/|L|$ . In the thermodynamic potential (5), besides the standard uniaxial-anisotropy invariants  $\frac{1}{2}a\gamma_z^2$  and  $\frac{1}{2}bm_z^2$ , the exchange-energy invariants  $\frac{1}{2}Bm^2$  and  $\frac{1}{2}D(\gamma m)^2$ , and the Dzyaloshinskii field  $q(\gamma_x m_y - \gamma_y m_x)$ , we also take into account the relativistic exchange invariant  $\frac{1}{2}Rm^2\gamma_z^2$  and the doubly relativistic Dzyaloshinskii-field and uniaxial-anisotropy invariants  $r(\gamma_x m_y - \gamma_y m_x)\gamma_z^2$  and  $\frac{1}{4}f\gamma_z^4$  respectively. The following need, however, be said about the form of the thermodynamic potential (5): in (5) we have included the terms responsible for the isotropic departure of the antiferromagnetic vector from the plane perpendicular to  $C_3$ , but a unique determination of all the coefficients from our experiment is difficult, and therefore we shall, for simplicity of the theoretical analysis, take only the doubly relativistic uniaxial-anisotropy invariant [6] into account. The changes that the neglected invariants introduce will be considered at the end of the paper. We shall, in the theoretical analysis, also take into account the fact that when  $H \perp C_3$  the antiferromagnetic vector  $L$  lies in the plane perpendicular to the magnetic field, i.e.,  $\gamma \cdot m = 0$ .

Thus, taking the foregoing into consideration, going over to polar coordinates, and minimizing the thermodynamic potential (5) with respect to  $m$  and  $\theta$  ( $\theta$  is the angle between the direction of the antiferromagnetic

vector  $\mathbf{L}$  and the axis  $C_3$ ), we obtain for  $\mathbf{H} \perp C_3$  ( $\mathbf{H} \parallel [010]$ ) the following expressions for the magnetization:

$$M_x=0, \quad M_y = \frac{q}{B} \sin \theta + \frac{H}{B}, \quad M_z=0 \quad (6)$$

and the equation for the change in the quantity  $\theta$  upon increase of the magnetic field  $\mathbf{H} \parallel [010]$ :

$$\left\{ -\left( a + \frac{q^2}{B} + f \right) \sin \theta + f \sin^3 \theta \right\} + \left( 1 - \frac{\chi_{\parallel}}{\chi_{\perp}} \right) \frac{H^2}{B} \sin \theta \sin^2 \varphi \cos \theta = \frac{q}{B} H \cos \theta, \quad (7)$$

where  $1 - \chi_{\parallel}/\chi_{\perp} = D/B + D$ .

The thermodynamic potential (5) as a function of the angle  $\theta$  and the magnetic field  $\mathbf{H}$  then has the form

$$\Phi = \frac{1}{2} a \cos^2 \theta - \frac{1}{2} \frac{q^2}{B} \sin^2 \theta - \frac{q}{B} (H_y \cos \varphi - H_x \sin \varphi) \sin \theta + \frac{1}{4} f \cos^4 \theta + \frac{1}{2} \frac{D}{B+D} \frac{(\gamma \mathbf{H})^2}{B} - \frac{1}{2} \frac{H^2}{B} \quad (8)$$

( $\varphi$  is the angle between the direction of  $\mathbf{L}$  and a  $C_2$  axis).

The solutions to Eq. (7) for  $H=0$  are the angles satisfying the following relations:

$$\sin \theta = 0, \quad \cos \theta = 0, \quad Bf \cos^2 \theta = -a - q^2/B, \quad (9)$$

i.e., depending on the magnitudes of the constants entering into the thermodynamic potential (8) (for given values of the effective-field constants and for a given value of the magnetic field), there is realized that state which corresponds to the minimum of the thermodynamic potential (8)—the antiferromagnetic vector  $\mathbf{L}$  can have three positions. One of the solutions to (8) for  $H=0$  is such that the antiferromagnetic vector  $\mathbf{L}$  is inclined at an angle  $\theta_0$  to the trigonal axis and  $\mathbf{L} \perp \mathbf{H}$ , where the angle  $\theta_0$  is given by

$$\cos^2 \theta_0 = (-aB - q^2)/Bf. \quad (10)$$

When  $\mathbf{H} \perp C_3$ , we have  $\sigma_{D\perp} \parallel \mathbf{H}$  and  $\mathbf{L} \perp \mathbf{H}$ ; in this case  $\gamma \mathbf{m} = 0$  and  $\sin \varphi = 0$  in Eq. (7). For some field  $H = H_C$ ,  $\sin \theta_0 = 1$ , and we have from (7) and (9) the relation

$$Bf \cos^2 \theta_0 = qH_C = -aB - q^2. \quad (11)$$

Then Eq. (7) can be rewritten in the form

$$\sin^3 \theta - \sin^2 \theta_0 \sin \theta - (H/H_C) \cos^2 \theta_0 = 0. \quad (12)$$

This equation characterizes the change in the value of the angle  $\theta$  between the  $C_3$  axis and the antiferromagnetic vector  $\mathbf{L}$  when the magnetic field is changed in the interval  $0 \leq H \leq H_C$ . When  $H \geq H_C$ , the antiferromagnetic vector  $\mathbf{L}$  lies in the (001) plane, i.e.,  $\sin \theta = 1$ . Comparing the results of the experiment with the theory, we can conclude that the vector  $\mathbf{L}$  makes an angle  $\theta_0 = 68 \pm 2^\circ$  with the trigonal axis when  $H=0$  and  $T = 4.2^\circ \text{K}$ . The value of the angle is determined, according to (6), from the ferromagnetic-moment ratio:  $\sin \theta_0 = \sigma_{D\perp}^I / \sigma_{D\perp}^{II}$ . The obtained value of  $\theta_0$  is in fairly good agreement with the value  $\theta_0 = (62 \pm 10)^\circ$  obtained from Alikhanov's  $H=0$  neutron-diffraction data [2]. As the magnetic field  $\mathbf{H} \perp C_3$  is increased, the antiferromagnetic vector  $\mathbf{L}$  turns toward the (001) plane; the value of the ferromagnetic moment  $\sigma_{D\perp} \parallel \mathbf{H}$  increases in the process and the vector  $\mathbf{L}$  lies in the (001) plane when  $H > H_C$ .

When  $H=0$ , the position of the vector  $\mathbf{L}$  relative to

the crystal axes is restricted by symmetry conditions:  $\mathbf{L}$  lies in a symmetry plane of the crystal. On application of a magnetic field  $\mathbf{H}$  in the basal plane (001), however, the symmetry restrictions are removed and then the antiferromagnetic vector  $\mathbf{L} \perp \mathbf{H}$ . From the experimental results for  $H < H_C$  (the linear dependence  $M_{\parallel}(H)$ , Fig. 3) and the expression (6), we can conclude that the variation of the angle  $\theta$  as the magnetic field  $\mathbf{H}$  is increased is given by the expression

$$\sin \theta = \sin \theta_0 + (1 - \sin \theta_0) H/H_C.$$

This expression satisfies to a good degree of accuracy (to within 2%) Eq. (12), i.e., it is a solution to Eq. (12) as the magnetic field  $\mathbf{H}$  is increased. The form of such a solution is obtained if Eq. (12) is represented in the form

$$\sin \theta [\sin \theta - \sin \theta_0] [\sin \theta + \sin \theta_0] = (H/H_C) (1 - \sin \theta_0) (1 + \sin \theta_0), \quad (12')$$

and since the angle  $\theta_0$  determined by us for  $H=0$  is equal to  $(68 \pm 2)^\circ$ , we can, correct to 5%, replace Eq. (12') in this case by  $\sin \theta \approx 1$  and  $\sin \theta + \sin \theta_0 = 1 + \sin \theta_0$ . The nonlinearity of the field dependence of the magnetic moment obtained by solving the cubic equation (12) is then a few percent of the linear approximation, and the field dependence of the resultant magnetic moment is given by the expression

$$M_{\parallel}^I = \frac{q}{B} \sin \theta + \frac{q}{B} (1 - \sin \theta_0) \frac{H}{H_C} + \frac{H}{B}. \quad (13)$$

Comparing the expression (13) with (1), we find that for  $H \leq H_C$  the magnetic susceptibility  $\chi_{\perp}^I$  has the form

$$\chi_{\perp}^I = \frac{q}{B} (1 - \sin \theta_0) \frac{1}{H_C} + \frac{1}{B}. \quad (14)$$

For  $H > H_C$ ,  $\sin \theta = 1$ , and the field dependence of the resultant magnetic moment is given by the expression

$$M_{\parallel}^{II} = \frac{q}{B} + \frac{1}{B} H = \sigma_{D\perp} + \chi_{\perp}^{II} H,$$

i.e., the experimentally observed susceptibility

$$\chi_{\perp}^{II} = 1/B = \chi_{\perp} \quad (15)$$

is the magnetic susceptibility in the basal (001) plane, and  $\sigma_{D\perp}^{II} = \sigma_{D\perp}$ .

From the experimental data for  $H \geq H_C$  we can determine the magnitude of the exchange field:  $H_E = 320 \pm 40$  kOe and the magnitude of the Dzyaloshinskiĭ field:  $H_{D\perp} = \sigma_{D\perp} / \chi_{\perp} = 140 \pm 20$  kOe. Comparing the expressions (14) and (15) with (3), we obtain a relation between the effective fields:

$$\frac{H_{D\perp}}{H_C} (1 - \sin \theta_0) = \frac{\chi_{\perp}^I - \chi_{\perp}^{II}}{\chi_{\perp}^{II}} = 0.6,$$

which is satisfied to a good degree of accuracy by the given values of the effective fields  $H_{D\perp}$  and  $H_C = 14$  kOe and the value obtained for the angle  $\theta_0$ . Knowing the effective Dzyaloshinskiĭ field  $H_{D\perp}$ , the exchange field  $H_E$ , and the field  $H_C$  at which the turning of the antiferromagnetic vector toward the (001) plane is completed, we can obtain from the relation (11) the values of the effective uniaxial-anisotropy fields:

$$H_{AB}^I = \sqrt{aB} = 160 \pm 20 \text{ kOe} \quad H_{AB}^{II} = \sqrt{fB} = 138 \pm 20 \text{ kOe}.$$

It also follows from the expression (11) that in the thermodynamic potential (5) the sign of the first uniaxial-anisotropy invariant should be negative, while the second should be positive, i.e.,  $a < 0$  and  $f > 0$ . Then the minimum of the thermodynamic potential (8) for

$H < H_C$  corresponds to the state in which the antiferromagnetic vector  $\mathbf{L}$  makes some angle  $\theta_0$  with the direction of the trigonal axis; this angle is determined by Eq. (12) for  $H \neq 0$  and by the relation (10) for  $H = 0$ .

The inclination of  $\mathbf{L}$  at an angle of  $\theta$  to the trigonal axis is also corroborated by the data presented in Fig. 6 for the dependence  $M_{\perp}(H)$ . The coefficient  $A$ , which depends on the direction of  $\mathbf{L}$  relative to  $C_3$ , is different from unity (if  $A = 1$ , then  $\mathbf{L} \perp C_3$ ).

### Magnetic Field $\mathbf{H} \parallel C_3$

If  $\mathbf{H} \parallel C_3$ , then  $\gamma \cdot \mathbf{m} \neq 0$ . Then, minimizing the thermodynamic potential (5), we obtain an equation for the dependence of the angle  $\theta$  on the magnetic field:

$$\left(-a - \frac{q^2}{B} - f \cos^2 \theta - \frac{D}{B+D} \frac{H^2}{B}\right) \sin \theta \cos \theta = 0. \quad (16)$$

For  $H = 0$ , the solutions to this equation are also solutions to (9), and, consequently, the state in which  $\mathbf{L}$  is inclined at angle  $\theta_0$  to the trigonal axis  $C_3$  is realized when  $H = 0$ . For  $H \neq 0$ , the solution to Eq. (16) has the form

$$\cos^2 \theta = -\frac{aB + q^2}{Bf} - \frac{D}{B+D} \frac{H^2}{Bf},$$

i.e., we obtain that for  $\mathbf{H} \parallel C_3$

$$\cos^2 \theta = \cos^2 \theta_0 - \frac{D}{B+D} \frac{H^2}{Bf}. \quad (17)$$

The resultant magnetic moment along the trigonal axis is then given by the expression

$$M_z = \frac{H}{B} \left[ 1 - \frac{D}{B+D} \left( \cos^2 \theta_0 - \frac{D}{B+D} \frac{H^2}{Bf} \right) \right]. \quad (18)$$

Introducing the notation  $\chi_{\parallel} = 1/(B+D)$  and  $\chi_{\perp} = 1/B$ , we obtain

$$M_z = \chi_{\perp} H \left\{ 1 - \left[ 1 - \frac{\chi_{\parallel}}{\chi_{\perp}} \right] \left[ \cos^2 \theta_0 - \left( 1 - \frac{\chi_{\parallel}}{\chi_{\perp}} \right) \frac{H^2}{H_{\perp}^2} \right] \right\}. \quad (19)$$

Taking the relations (11) and (17) into account, we find that when the magnetic field  $\mathbf{H} \parallel C_3$ , the antiferromagnetic vector turns toward the (001) plane as the field  $H$  is increased from zero to  $H_C^{\text{II}}$ , where

$$H_C^{\text{II}} = \left( \frac{aB - q^2}{1 - \chi_{\parallel}/\chi_{\perp}} \right)^{1/2} = \left( \frac{H_{D\perp} H_C^{\text{I}}}{1 - \chi_{\parallel}/\chi_{\perp}} \right)^{1/2}.$$

when  $H > H_C^{\text{II}}$ , the vector  $\mathbf{L}$  lies in the (001) plane. The dependence of the resultant magnetic moment in the direction of the trigonal axis on the field for  $0 < H < H_C^{\text{II}}$  is given by the expression (19), while for  $H > H_C^{\text{II}}$  we have  $M_z = H/B = \chi_{\perp} H$ .

Notice that the analysis here is carried out without allowance for the anisotropy in the magnetic susceptibility  $\chi_{\perp}$  ( $\mathbf{H} \parallel C_3$  and  $\mathbf{H} \perp C_3$ ). Allowance for this anisotropy leads to a situation in which when  $\mathbf{L} \perp C_3$  ( $H > H_C^{\text{II}}$ ) and  $\mathbf{H} \parallel C_3$  the quantity  $\chi_{\perp}^* = 1/(B+b)$  ( $\chi_{\perp}$  in the expressions (18) and (19) should be replaced by  $\chi_{\perp}^*$ ), where the constant  $b$  corresponds to the invariant  $bm_z^2/2$  in the thermodynamic potential (5).

The experimentally obtained value for the magnetic susceptibility  $\chi_{\perp}^*$  for  $\mathbf{H} \parallel C_3$  is in satisfactory agreement with the expression (18) and the value obtained for the angle  $\theta_0$  if we allow for the fact that we neglected in the thermodynamic potential (5) the invariants corresponding to the anisotropy in the magnetic susceptibility for  $\mathbf{H} \perp C_3$  and  $\mathbf{H} \parallel C_3$ . The nonlinearity, given by

the formulas (18) and (19), of the dependence  $M_z(H)$  lies within the limits of the experimental error. It may, however, be inferred that the magnetic field  $H < H_C^{\text{II}}$  in our experiments.

### RESULTS OF THE THERMAL MEASUREMENTS (MAGNETIC FIELD PERPENDICULAR TO THE TRIGONAL AXIS)

As can be seen from Figs. 3 and 4, as the temperature is increased, the angle between the direction of the antiferromagnetic vector  $\mathbf{L}$  and the axis decreases, and the crystal becomes purely antiferromagnetic with  $\mathbf{L}$  directed along the trigonal axis: there is no weak ferromagnetism in this case. Such a variation of the position of the antiferromagnetic vector can be understood if we allow for the fact that as the temperature is increased, and near the transition point, the dominant role in the thermodynamic potential (5) is played by the effective first-order anisotropy fields, and since the constant of the effective field of the uniaxial anisotropy in the invariant  $a\gamma_z^2/2$  is less than zero, the crystal can be in the purely antiferromagnetic state near the transition point. The antiferromagnetic vector  $\mathbf{L}$  is then directed along the trigonal axis  $C_3$ .

The nature of the variation of the angle  $\theta_0$  with temperature can be understood by comparing the obtained result with the expression (10) for the dependence of the angle  $\theta_0$  on the thermodynamic values of the effective anisotropy fields, assuming for simplicity in doing this that the anisotropy constants entering into the thermodynamic potential (5) are temperature independent. The  $T$  dependence of the effective fields, however, is determined by the temperature dependence of the antiferromagnetic vector  $\mathbf{L}$ , i.e.,

$$aB = a^* B l^2, \quad q = q^* l, \quad Bf = Bf^* l^2; \quad l = L(T)/L(0).$$

Therefore, the quantity  $(a^*B - q^{*2})/Bf^* l^2$ , which, as we have shown, is equal to 0.12 at liquid-helium temperatures ( $l = 1$ ), should increase with temperature, and will, at some temperature  $T_I$ , be equal to

$$\frac{a^*B - q^{*2}}{Bf^* l^2} = \cos^2 \theta_1 = 1,$$

i.e., at the temperature  $T_I$  we have  $l^2(T_I) = (a^*B - q^{*2})/Bf^* = 0.12$ , and the antiferromagnetic vector gets aligned along the trigonal axis. The crystal then ceases to be weakly ferromagnetic, becoming purely antiferromagnetic.

Figure 7 shows the plot of the function  $[\sigma_{D\perp}(T)/\sigma_{D\perp}(0)]^2$  obtained from the temperature dependence of  $\sigma_{D\perp}$  (the quantity  $\sigma_{D\perp}(T) = \sigma_{D\perp}^{\text{II}}(T)$  depends

linearly on  $L(T)$ ). At  $T = 23.4 \pm 0.5$  °K,  $[\sigma_{D\perp}(T)/\sigma_{D\perp}(0)]^2 = 0.12$ . Thus, in such a simplified model the purely antiferromagnetic state should be realized at  $T_I \geq 23.4 \pm 0.5$  °K. In our experiments the antiferromagnetic state without weak ferromagnetism arises at  $T_I^{\text{exp}} \geq 22.6 \pm 0.5$  °K.

Figure 8 shows the dependence on temperature for  $H = 0$  of the angle  $\theta_0$  between the antiferromagnetic vector  $\mathbf{L}$  and the trigonal axis  $C_3$ . The values of  $\theta_0(T)$  were determined from the ratio  $\sin \theta_0(T) = \sigma_{D\perp}^{\text{I}}(T)/\sigma_{D\perp}^{\text{II}}(T)$ , which was taken from the experiment (Figs. 3 and 4). The same figure shows a plot of  $\theta_0(T)$  obtained theoretically on the basis of the formula (17) and the function  $\gamma^2(T)$ . The qualitative agreement of the experiment with the considered model is apparent.

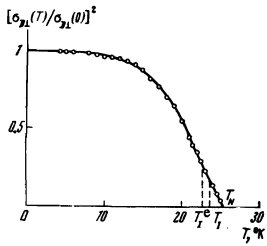


FIG. 7

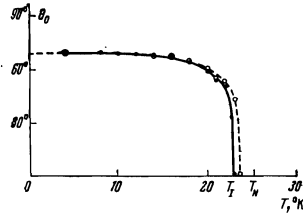


FIG. 8

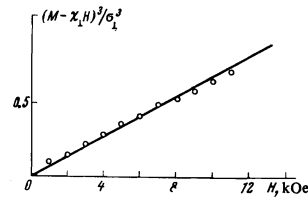


FIG. 9

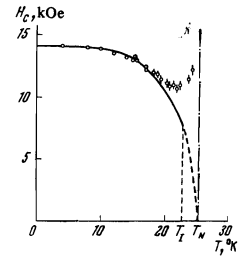


FIG. 10

FIG. 7. The temperature dependence of the square of the ratio of the ferromagnetic moments, which is proportional to  $[L(T)/L(0)]^2$ , the square of the ratio of the antiferromagnetic vectors.

FIG. 8. The temperature dependence of the angle between the antiferromagnetic vector  $L$  and the trigonal axis  $C_3$ . The values represented by black circles were obtained from the ratio of the ferromagnetic moments, those represented by light circles from the expression (17).

As the magnetic field  $H \perp C_3$  is increased from zero intensity, the antiferromagnetic vector  $L$  turns toward the (001) plane, the dependence of the angle  $\theta$  on the magnetic field being also given by Eqs. (7) and (12). It should, however, be noted that it is possible that  $\gamma_m \neq 0$  ( $\sin \varphi \neq 0$ ) at these temperatures, since as the temperature increases and approaches  $T_N$  the longitudinal magnetic susceptibility  $\chi_{||}$  becomes comparable to the transverse magnetic susceptibility  $\chi_{\perp}$ , and it is necessary to consider in Eqs. (7) and (12) the term

$$\left(1 - \frac{\chi_{||}}{\chi_{\perp}}\right) \frac{H^2}{H_{AB}^2} \sin \theta \sin^2 \varphi. \quad (20)$$

As the angle  $\theta_0$  decreases, it increasingly becomes inadmissible to approximate the solution to these equations by a linear function of  $\sin \theta$ . Therefore, as the temperature increases (as it approaches  $T_I$  and above this temperature), the linear low-field sections of the  $M_{||}(H)$  curves vanish. At the temperature  $T_I = 22.6^\circ \text{K}$ , when  $\sin^2 \theta_0 = 0$ , Eq. (12) assumes the form  $\sin^3 \theta = H/H_C$ , and the field dependence of the magnetic moment is given by the formula

$$M_{||}(H) = \sigma_{D\perp}(T) \sin \theta + \chi_{\perp} H = \sigma_{D\perp}(T) (H/H_C)^{1/3} + \chi_{\perp} H.$$

Figure 9 shows the magnetic-field dependence of the quantity  $(M_{||} - \chi_{\perp} H)^3$ . It can be seen from the figure that the theoretical  $H$  dependence of  $M_{||}$  in this case is in good agreement with experiment. The observed discrepancy at high  $H$  can be explained by the presence in Eq. (7) of a term connected with the longitudinal magnetic susceptibility.

Figure 10 shows the temperature dependence of the magnetic field  $H_C$  at which the turning of the antiferromagnetic vector  $L$  toward the (001) plane is completed. The quantity  $H_C(T)$  was determined from the shift of the kink in the magnetization curve  $M_{||}(H)$  as the temperature was increased to the temperature  $T_I$  and from the end of the nonlinear section of  $M_{||}(H)$  in the range  $T_I < T < T_N$ . As follows from Fig. 10, for  $T \ll T_N$ ,  $H_C(T)$  decreases in proportion to  $L(T)$  (the continuous curve), which is confirmed by the results of the theory—see (8)—for  $L \perp H$  ( $\sin \varphi = 0$ ). At high temperatures, however, the curve  $H_C(T)$  does not coincide with  $L(T)$ , which can be explained by the presence in (7) of the term (20). Since  $\chi_{||}$  becomes comparable to  $\chi_{\perp}$  as the temperature is increased, and  $\varphi$  may not be equal to zero, allowance for this term in (7) leads to an increase in  $H_C(T)$ . It should, however, be noted that the determination of  $H_C(T)$  and the discussion of the results are made difficult by the nonlinearity of the dependence  $M_{||}(H)$ .

FIG. 9. The magnetic-field dependence of the difference  $(M_{||} - \chi_{\perp} H)^3$ , obtained from the curve  $M_{||}(H)$  at  $T = 22.6^\circ \text{K}$ .

FIG. 10. The temperature dependence of the magnetic field  $H_C$  at which the turning of  $L$  toward the (001) plane is completed.

### The Thermal Measurements with $H \parallel C_3$

The magnetic-field dependence of the magnetic moment  $M_{||}(H)$  of the sample at different temperatures is, if the magnetic field is directed along the trigonal axis, linear:  $M_{||}(H) = \chi_{\perp}^*(T)H$ , and, evidently, the value of the magnetic field

$$H_c^{II} = \left[ \frac{H_{AB}^2 - H_{D\perp}^2}{1 - \chi_{||}/\chi_{\perp}} \right]^{1/2},$$

at which the turning of  $L$  toward the (001) plane is completed, does not depend on temperature, as follows from the expression for  $H_c^{II}$ . The dependence  $\chi_{\perp}^*(T)$  for  $H \parallel C_3$  is shown in Fig. 5.

Concerning the relativistic exchange invariant  $\frac{1}{2} R m^2 \gamma_D^2$  and the doubly-relativistic Dzyaloshinskii-field invariant  $r(\gamma_X m_Y - \gamma_Y m_X) \gamma_D^2$ , which are neglected in the thermodynamic potential (5), we can say the following: allowance for them in (5) complicates the expressions for the spontaneous magnetic moment and the magnetic susceptibility for  $H < H_C$ , and makes the determination of the angle  $\theta_0$  between the antiferromagnetic vector  $L$  and the trigonal axis  $C_3$  difficult. Minimizing the thermodynamic potential (5), we obtain for  $\sigma_{D\perp}$  and  $\chi_{\perp}$  the expressions

$$\sigma_{D\perp}^{II} = \frac{q + r\gamma_D^2}{B + R\gamma_D^2} \gamma_{\perp}, \quad \chi_{\perp}^{II} = \frac{1}{B + R\gamma_D^2}; \quad \sigma_{D\perp}^{II} = \frac{q}{B}, \quad \chi_{\perp}^{II} = \frac{1}{B},$$

as well as the expressions for  $H_C$  and  $\cos^2 \theta_0$  in terms of the allowed-for constants:

$$\cos^2 \theta_0 = \frac{-aB - q^2 + 2qr - q^2 R/B}{2aR + 4qr - 2r^2 + Bf};$$

$$H_c = \frac{-aB - q^2 + 2qr - q^2 R/B}{q - 2r + 2qR/B}.$$

The main experimental results that the antiferromagnetic vector  $L$  is inclined at an angle  $\theta_0 = (68 \pm 2)^\circ$  to the trigonal axis at  $T = 4.2^\circ \text{K}$  and  $H = 0$  and lies in the plane perpendicular to  $C_3$  when  $H \geq H_C = 14 \text{ kOe}$ , however, remain unchanged; as the temperature is increased (when  $H = 0$ ), the vector  $L$  turns toward the trigonal axis, and is directed along the trigonal axis  $C_3$  (absence of weak ferromagnetism) when  $T > 22.6^\circ \text{K}$ .

Let us consider the behavior of the magnetic susceptibility near  $T_N$ . The temperature dependence of the magnetic susceptibility  $\chi_{\perp}$  for  $H \perp C_3$  and  $T \leq T_N$  (Fig. 5) is given by the formula

$$\chi_{\perp}(T) = \chi_{\perp}(0) \left(1 - \frac{A}{T_N - T}\right), \quad (21)$$

where  $A = 1.6 \pm 0.3$ , and, for  $T \geq T_N$ , has the form

$$\chi_{\perp}(T) = \chi_{\perp}(0) \left[1 - \frac{B}{T - T_N}\right] \quad (22)$$

where  $B = 2.7 \pm 0.3$ . It can be seen from the relations (21) and (22) that the conclusions of the thermodynamic theory<sup>[9]</sup> about the dependence  $\chi_{\perp}(T)$  near the critical point for the transition to the antiferromagnetic state with weak ferromagnetism are realized:  $B \approx 2A$ .

## CONCLUSION

Thus, it has been experimentally demonstrated in this work that at  $T = 4.2$  °K and  $H = 0$  there is realized in  $\text{NiCO}_3$  a state in which the antiferromagnetic vector  $\mathbf{L}$  is inclined at an angle  $\theta_0 = (68 \pm 2)^\circ$  to the trigonal axis. As the field  $\mathbf{H} \perp C_3$  is increased from zero intensity, the antiferromagnetic vector  $\mathbf{L}$  turns toward the (001) plane and lies in that plane when  $H > H_C = 14$  kOe. In this case the magnitude of the spontaneous magnetic moment  $\sigma_{D\perp} = 2340 \pm 40$  emu/mole and the magnetic susceptibility  $\chi_{\perp} = (16.8 \pm 1) \times 10^{-3}$  emu/mole. The values of the magnetic susceptibility  $\chi_{\perp}$  and the spontaneous magnetic moment  $\sigma_{D\perp}$  correspond to an exchange field  $H_E = 320 \pm 40$  kOe and a Dzyaloshinskii field  $H_{D\perp} = 140 \pm 20$  kOe. It has been shown that the departure of  $\mathbf{L}$  from the basal plane can be explained by the fact that the fourth-order uniaxial-anisotropy constant is comparable in magnitude to the second-order uniaxial-anisotropy constants  $H_{AE}$  and  $H_{AE}^{\text{II}}$ .

As the temperature is increased when  $H = 0$ , the crystal  $\text{NiCO}_3$  goes over into a purely antiferromagnetic state with the antiferromagnetic vector directed along the trigonal axis. The crystal then possesses no spontaneous magnetic moment. The temperature dependence of the angle  $\theta_0$  between the antiferromagnetic vector and the trigonal axis has been determined. It is shown that the function  $\theta_0(T)$  is determined by the tem-

perature dependence of the effective anisotropy fields  $H_{AE}$ ,  $H_{AE}^{\text{II}}$ , and  $H_{D\perp}$ .

As the magnetic field  $\mathbf{H} \perp C_3$  is increased from zero intensity at different temperatures, the antiferromagnetic vector turns toward the (001) plane. The dependence  $H_C(T)$  has been determined.

The author thanks P. L. Kapitza for constant interest in the work. He is sincerely grateful to A. S. Borovik-Romanov and N. M. Kreines for supervising the work and for a discussion of the results and to I. E. Dzyaloshinskii for a discussion of the results.

<sup>1)</sup>The author sincerely thanks A. A. Shternberg and Yu. M. Minenzon for kindly placing the crystals at his disposal

<sup>1)</sup>H. Bizette and B. Tsai, C. R., Paris, 241, 546 (1955).

<sup>2)</sup>R. A. Alikhanov, J. Phys. Soc. Japan 17, Suppl. B-111, 58 (1962).

<sup>3)</sup>I. E. Dzyaloshinskii, Zh. Eksp. Teor. Fiz. 32, 1547 (1957) [Sov. Phys.-JETP 5, 1259 (1957)].

<sup>4)</sup>L. A. Prozorova, Zh. Eksp. Teor. Fiz. 57, 1967 (1969) [Sov. Phys.-JETP 30, 1065 (1970)].

<sup>5)</sup>N. M. Kreines and T. A. Shal'nikova, Zh. Eksp. Teor. Fiz. 58, 522 (1970) [Sov. Phys.-JETP 31, 280 (1970)].

<sup>6)</sup>Yu. M. Minenzon and L. I. Ivanov, Neorgan. Mater. (1974).

<sup>7)</sup>S. Foner, Rev. Sci. Inst. 30, 548 (1959).

<sup>8)</sup>R. Z. Levitin and V. A. Shurov, ZhETF Pis. Red. 7, 142 (1968) [JETP Lett. 7, 110 (1968)].

<sup>9)</sup>A. S. Borovik-Romanov and V. I. Ozhogin, Zh. Eksp. Teor. Fiz. 39, 27 (1960) [Sov. Phys.-JETP 12, 18 (1961)].

Translated by A. K. Ageyi

112